# MULTISCALE MODELLING OF THE TEXTILE COMPOSITE MATERIALS

**\*Zahur Ullah, Łukasz Kaczmarczyk, Michael Cortis and Chris J. Pearce**

School of Engineering, Rankine Building, The University of Glasgow, Glasgow, UK, G12 8LT

\*Zahur.Ullah@glasgow.ac.uk

## ABSTRACT

This paper presents an initial computational multiscale modelling of the fibre-reinforced composite materials. This study will constitute an initial building block of the computational framework, developed for the DURCOMP (providing confidence in durable composites) EPSRC project, the ultimate goal of which is the use of advance composites in the construction industry, while concentrating on its major limiting factor "durability". The use of multiscale modelling gives directly the macroscopic constitutive behaviour of the structures based on its microscopically heterogeneous representative volume element (RVE). The RVE is analysed using the University of Glasgow in-house parallel computational tool, MoFEM (Mesh Oriented Finite Element Method), which is a C++ based finite-element code. A single layered plain weave is used to model the textile geometry. The geometry of the RVE mainly consists of two parts, the fibre bundles and matrix, and is modelled with CUBIT, which is a software package for the creation of parameterised geometries and meshes. Elliptical cross sections and cubic splines are used respectively to model the cross sections and paths of the fibre bundles, which are the main components of the yarn geometry. In this analysis, transversely isotropic material is introduced for the fibre bundles, and elastic material is used for the matrix part. The directions of the fibre bundles are calculated using a potential flow analysis across the fibre bundles, which are then used to define the principal direction for the transversely isotropic material. The macroscopic strain field is applied using linear displacement boundary conditions. Furthermore, appropriate interface conditions are used between the fibre bundles and the matrix.

**Key Words:** *multiscale modelling; composite material; Transverse isotropy; MoFEM; CUBIT*

## 1. Introduction

Conventional materials, e.g. steel, aluminium and metallic alloys can no longer satisfy the demands for materials with exceptional mechanical properties and ultimately requires the design of new material [1]. These new materials are designed by changing their microconstituents at a scale, which is very small as compared to the physical structures. Due to the complicated micro-structure of these materials, direct macro-level modelling is not possible and requires a detailed modelling at the micro-level. Textile or fabric composites is a class of these new materials which provides full flexibility of design and functionality due to the mature textile manufacturing industry and is commonly used in many engineering applications, including ships, aircrafts, automobiles, civil structures and prosthetics [2]. Numerous analytical and computational methods have been proposed to analyse textile composite materials, which includes the calculation of the overall macro homogenised response and properties from the micro-heterogeneous representative value element (RVE) [3] and is often referred as micro-to-macro transition or homogenisation [4].

This paper presents the computational multiscale modelling of the textile composites, using the University of Glasgow in-house computational tool MoFEM. The RVE in this case consists of fibre bundles and matrix, which is modelled and meshed in CUBIT using a Python parametrized script. CUBIT also facilitates the insertion of interfaces between the fibres and matrix. Transversely isotropic material are used for the fibres and isotropic martial are used for the matrix. Five material parameters are required

for the transversely isotropic material, i.e. $E_p$, $\nu_p$, $E_z$, $\nu_{pz}$ and $G_{zp}$ where $E_p$ and $\nu_p$ are Young's modulus and Poisson's ratio in the transverse direction respectively, while $E_z$, $\nu_{pz}$ and $G_{zp}$ are the Young's modulus, Poisson's ratio and shear modulus in the fibre directions respectively. For the matrix part, only two material parameters are required, i.e. Young's modulus $E$ and Poisson's ratio $\nu$. Although, periodic boundary conditions [5, 6] gives better estimates of the homogenised response and properties as compared to traction and linear displacement boundary conditions, linear displacement boundary conditions are used in this paper due to its simple implementation. This will subsequently be extended to periodic boundary conditions in future work. Fibre directions are calculated at each integration point by solving a potential flow problem.

## 2. Theoretical background

Computational multiscale modelling is used in this paper to analyse the textile composite materials, in which a heterogeneous RVE is associated with each integration point of the macro-homogenous structure as shown in Figure 1, in which $\overline{B} \subset \mathbb{R}^3$ and $B \subset \mathbb{R}^3$ are macro and micro domains respectively. The calculation of the RVE boundary conditions from the macro-strain
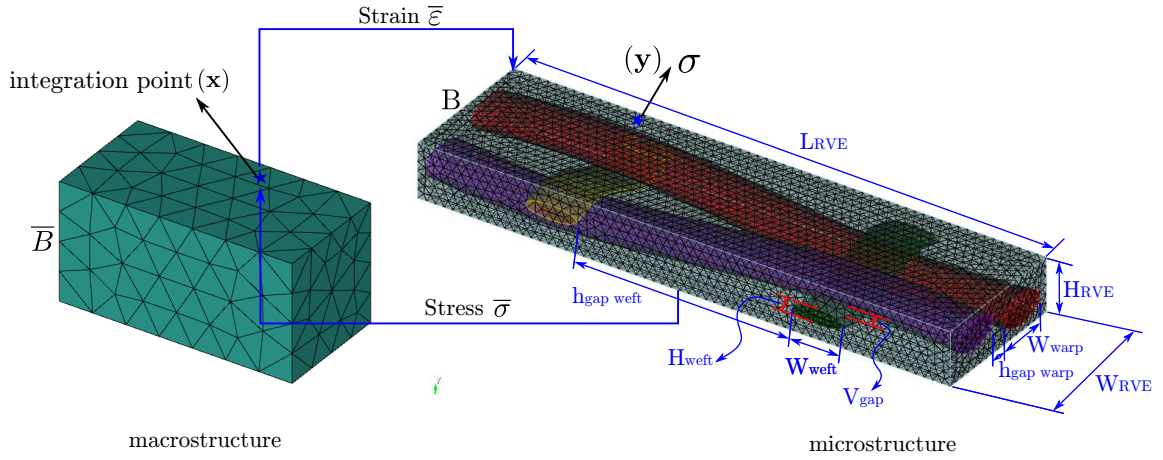


Figure 1: Transition from macro-to-micro and micro-to-macro

$\overline{\varepsilon} = \begin{bmatrix} \overline{\varepsilon}_{11} & \overline{\varepsilon}_{22} & \overline{\varepsilon}_{33} & 2\overline{\varepsilon}_{12} & 2\overline{\varepsilon}_{23} & 2\overline{\varepsilon}_{31} \end{bmatrix}^T$ at macroscopic integration point $\mathbf{x} = \begin{bmatrix} x_1 & x_2 & x_3 \end{bmatrix}^T$ is known as macro-to-micro transition, while subsequent calculation of the homogenised stress $\overline{\sigma} = \begin{bmatrix} \overline{\sigma}_{11} & \overline{\sigma}_{22} & \overline{\sigma}_{33} & \overline{\sigma}_{12} & \overline{\sigma}_{23} & \overline{\sigma}_{31} \end{bmatrix}^T$ and tangent moduli is known as micro-to-macro transition. The macro-strain is applied as linear displacement boundary conditions, which leads to satisfaction of Hill-Mandel principle [7], i.e.

$$\overline{\varepsilon} : \overline{\sigma} = \frac{1}{V} \int_V \varepsilon : \sigma \, dV, \tag{1}$$

where $V$ is the volume of the RVE, while $\sigma$ and $\varepsilon$ are stresses and strains associated with a point $\mathbf{y} = \begin{bmatrix} y_1 & y_2 & y_3 \end{bmatrix}^T$ of the RVE. The micro displacement field $\mathbf{u} = \begin{bmatrix} u_1 & u_2 & u_3 \end{bmatrix}^T$, is written as

$$\mathbf{u} = \mathbf{u}^* + \widetilde{\mathbf{u}}, \tag{2}$$

where $\mathbf{u}^*$ is known as Taylor displacements and $\widetilde{\mathbf{u}}$ is the unknown displacement fluctuations. The Taylor component is written as

$$\mathbf{u}_i^* = \mathbb{D}_i^T \overline{\varepsilon}, \qquad i = 1, 2, \cdots n, \tag{3}$$

where $n$ is the number of nodes and $\mathbb{D}_i$ is the coordinate matrix and is given as [4]

$$\mathbb{D}_i = \frac{1}{2} \begin{bmatrix} 2y_1 & 0 & 0 \\ 0 & 2y_2 & 0 \\ 0 & 0 & 2y_3 \\ y_2 & y_1 & 0 \\ 0 & y_3 & y_2 \\ y_3 & 0 & y_1 \end{bmatrix}_i. \tag{4}$$

Finally, the homogenised stress is calculated as

$$\overline{\boldsymbol{\sigma}} = \frac{1}{V} \sum_{i=1}^{n_b} \mathbb{D}_i \mathbf{f}_i^{ext}, \tag{5}$$

where $n_b$ is the number of nodes on the boundary $\partial B$ of the RVE, and $\mathbf{f}_i^{ext}$ is the external nodal force vector.

## 3. Numerical example

A sample RVE, which was used in [2], is used here with the same geometrical and material parameters, as shown in Figure 1, where the subscripts warp and weft represent the corresponding directions of fibre bundles. The geometrical and material parameters are defined in Table 1. This RVE is referred

| Parameters | Values | Parameters | Values |
|---|---|---|---|
| $W_{warp}$ | 0.3 | $W_{weft}$ | 0.3 |
| $H_{warp}$ | 0.1514 | $H_{weft}$ | 0.0757 |
| $h_{gap\,warp}$ | 0.09 | $h_{gap\,weft}$ | 1.2 |
| $L_{RVE}$ | 3.0 | $v_{gap}$ | 0.012 |
| $W_{RVE}$ | 0.8 | | |
| $H_{RVE}$ | 0.3 | | |

| Fibres properties | | | | | Matrix Properties | |
|---|---|---|---|---|---|---|
| $E_p$ | $E_z$ | $v_p$ | $v_z$ | $G_{pz}$ | $E$ | $v$ |
| 40 | 270 | 0.26 | 0.26 | 24 | 35 | 0.35 |

Table 1: REV geometrical and material properties (all dimensions in mm while $E$ and $G$ are in $GPa$)



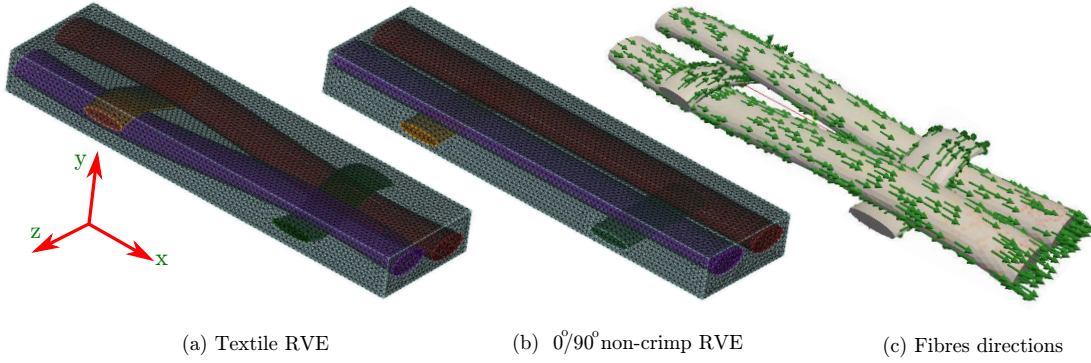(a) Textile RVE     (b) $0^o/90^o$ non-crimp RVE     (c) Fibres directions

Figure 2: Crimp and non-crimp RVEs and sample fibre directions

as unbalanced, where the dimensions of fibre bundles are different in warp and weft directions. The manufacturing processes and crossing of the warp and weft yarn will lead to non-circular cross sections of the fibre bundles; therefore, elliptical cross sections are used in this paper, which are then swept over the cubic spline fibres' path to generate the fibres. Four-node tetrahedral elements are used for both the fibre bundles and the matrix, while six-nodes prism elements are used as an interface between fibres and matrix.

The textile RVE is analysed using two different meshes with 41,193 and 106,011 DOFs and is subjected to 1 % strain in $x$ direction, i.e. $\overline{\varepsilon}_{xx}$. The finest mesh and coordinates system are shown in Figure 2(a), where $x$ and $z$ are warp and weft directions respectively, while sample fibre directions vector are shown in Figure 2(c). The resulting homogenised stress $\overline{\sigma}_{xx}$ versus applied strain $\overline{\varepsilon}_{xx}$ for the two meshes and a reference value from [2] are shown in Table 2, in which Mesh-2 with 106,011 DOFs provides satisfactory results. The small difference between current and reference results may be due to the use of lenticular cross-sections for the fibres, use of 8-node 3D linear brick element and 4- node linear tetrahedron element for fibres and matrix respectively and the use of perfect bonding between fibres and matrix in [2]. Furthermore, The effect of fibres dimensions and crimp pattern are analysed, for which a new $0^o/90^o$ non-crimp RVE with 103,095 DOFs (shown in Figure 2(b)) is generated and is subjected to the same strain state. Comparison of the homogenised stress $\overline{\sigma}_{xx}$ for both crimp and non-crimp RVEs are given in Table 3, where relatively lower value of homogenised stresses $\overline{\sigma}_{xx}$ in the crimp RVE is due to the waviness of the fibre bundles. Furthermore, both crimp and non-crimp RVEs are subjected to 1 % strain in $z$ direction, i.e. $\overline{\varepsilon}_{zz}$ and comparison of their homogenised stress in the $z$ direction, i.e. $\overline{\sigma}_{zz}$ are shown in

Table 3, where again $\overline{\sigma}_{zz}$ is lower for the crimp RVE. Due to the small size and higher waviness of the weft fibre bundles, the values of $\overline{\sigma}_{zz}$ are relatively smaller than the corresponding values of $\overline{\sigma}_{xx}$.

| | $\overline{\sigma}_{xx}$ (MPa) | | |
|---|---|---|---|
| $\overline{\varepsilon}_{xx}$ (%) | Mesh-1 | Mesh-2 | Reference |
| 1 | 749.82 | 508.771 | 541.278 |

<div align="center">Table 2: $\overline{\sigma}_{xx}$ versus $\overline{\varepsilon}_{xx}$ for different mesh levels</div>

| | $\overline{\sigma}_{xx}$ (MPa) | | | | $\overline{\sigma}_{zz}$ (MPa) | |
|---|---|---|---|---|---|---|
| $\overline{\varepsilon}_{xx}$ (%) | Crimp | Non-Crimp | | $\overline{\varepsilon}_{zz}$ (%) | Crimp | Non-Crimp |
| 1 | 508.771 | 751.507 | | 1 | 83.9317 | 125.065 |

<div align="center">Table 3: Comparison of $\overline{\sigma}_{xx}$ versus $\overline{\varepsilon}_{xx}$ and $\overline{\sigma}_{zz}$ versus $\overline{\varepsilon}_{zz}$ for crimp and non-crimp RVE</div>

## 4. Conclusions

This paper described an initial computational modelling framework for the DURACOMP project. Textile composite RVE geometry, which consists of two parts, i.e. fibre bundles and matrix is modelled and meshed using CUBIT, where fibres are modelled using cubic spline with elliptical cross sections. The University of Glasgow in-house computational tool MoFEM is used to analyse the RVE using transversely isotropic material for the fibre bundles and isotropic material for the matrix. Linear displacement boundary conditions and elastic interfaces between fibre bundles and matrix are used in this paper. Direction of the fibre bundles are calculated using a potential flow analysis. Two different level of meshes are used to solve the RVE, and it is found that the homogenised stress calculated in the case of Mesh-2 are in a good agreement with the reference solution. It is also found that homogenised stress in the case of the crimp RVE is lower than the corresponding non-crimp RVE. Furthermore, it is also observed that due to the relatively smaller dimensions and more waviness pattern for the weft fibre bundles, the homogenised stress $\overline{\sigma}_{zz}$ is lower than the corresponding stress $\overline{\sigma}_{xx}$ in the warp direction.

## Acknowledgements

## References

[1] D. Perić, E.A. de Souza Neto, A.J. Carneiro Molina, and M. Partovi. *Computational Methods in Applied Sciences*, volume 7, pages 165–185. Springer Netherlands, 2007.

[2] T. W. Chua. Multi–scale modeling of textile composites. Master's thesis, Department of Mechanical Engineering, Technische Universiteit Eindhoven, January 2011.

[3] V.G. Kouznetsova. *Computational homogenization for the multi-scale analysis of multi-phase materials*. PhD thesis, Technische Universiteit Eindhoven, The Netherlands, 2002.

[4] C. Miehe and A. Koch. Computational micro-to-macro transitions of discretized microstructures undergoing small strains. *Archive of Applied Mechanics*, 72(4-5):300–317, 2002.

[5] Ł. Kaczmarczyk, C. J. Pearce, and N. Bićanić. Scale transition and enforcement of RVE boundary conditions in second-order computational homogenization. *International Journal for Numerical Methods in Engineering*, 74(3):506–522, 2008.

[6] G. Soni, R. Singh, M. Mitra, and B. G. Falzon. Modelling matrix damage and fibre-matrix interfacial decohesion in composite laminates via a multi-fibre multi-layer representative volume element (M$^2$RVE). *International Journal of Solids and Structures*, 51(2):449 – 461, 2014.

[7] R. Hill. On constitutive macro-variables for heterogeneous solids at finite strain. In *Proceedings of the Royal Society of London. Series A, Mathematical and Physical Sciences*, volume 326, pages 131–147. The Royal Society, 1972.